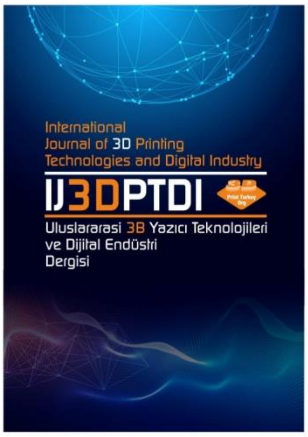

ULUSLARARASI 3B YAZICI TEKNOLOJİLERİ VE DİJİTAL ENDÜSTRİ DERGİSİ

INTERNATIONAL JOURNAL OF 3D PRINTING TECHNOLOGIES AND DIGITAL INDUSTRY

ISSN:2602-3350 (Online)

URL: https://dergipark.org.tr/ij3dptdi

AN EXPERIMENTAL INVESTIGATION ON THE EFFECT OF TEST SPEED ON THE TENSILE PROPERTIES OF THE PETG PRODUCED BY ADDITIVE MANUFACTURING

Yazarlar (Authors): Berkay Ergene*, Cagin Bolat

Bu makaleye şu şekilde atıfta bulunabilirsiniz (To cite to this article): *Ergene B., Bolat Ç., "An Experimental Investigation On The Effect Of Test Speed On The Tensile Properties of The Petg Produced By Additive Manufacturing" Int. J. of 3D Printing Tech. Dig. Ind., 6(2): 250-260, (2022).*

DOI: 10.46519/ij3dptdi.1069544

Araştırma Makale/ Research Article

Erişim Linki: (To link to this article): https://dergipark.org.tr/en/pub/ij3dptdi/archive

AN EXPERIMENTAL INVESTIGATION ON THE EFFECT OF TEST SPEED ON THE TENSILE PROPERTIES OF THE PETG PRODUCED BY ADDITIVE MANUFACTURING

Berkay Ergene[a]*, Cagin Bolat[b]

[a]Pamukkale University, Technology Faculty, Mechanical Engineering Department, TURKEY
[b]Istanbul Technical University, Machine Faculty, TURKEY

* *Corresponding Author:* bergene@pau.edu.tr

(**Received:** 07.02.2022; **Revised:** 25.04.2022; **Accepted:** 03.08.2022)

ABSTRACT

Additive manufacturing (AM) is a highly popular, versatile, and practical production technique due to its great ability of very fast prototyping. Compared to other traditional ways, the number of studies on AM techniques has increased in a noteworthy manner day by day on account of their promising potential for future works. In this paper, fused deposition modeling (FDM) technology was used to fabricate polyethylene terephthalate glycol (PETG) specimens and to analyze the effect of the test speed on their tensile properties. As for the printing parameters, solely layer thickness values (0.1 mm, 0.2 mm, and 0.4 mm) were altered while the other factors were kept constant. In order to ascertain the production effectiveness, hardness and surface roughness measurements were carried out. Uniaxial tensile tests were performed at three different test speeds: 5 mm/min, 25 mm/min, and 50 mm/min. Furthermore, after deformation inspections were conducted both in macro and micro scales to evaluate the failure better. From the damage analyses, it was seen that ductile dominant mixed type failure is valid for lower test speeds even though brittle dominant mixed type failure is detected for 50 mm/min test speed.

Keywords: PETG, Additive Manufacturing, Test Speed, Tensile Strength, Damage Mechanism.

1. INTRODUCTION

Additive manufacturing (AM), or in other words three-dimensional (3D) printing methodology, is a well-known and extremely versatile technique due to its perfect capability of rapid prototyping. By way of this technology, lots of prototype design can be easily obtained from the computer aided design (CAD) model data [1]. In addition, certain system components can also be fabricated through 3D printing in order to make rapid maintenance or to perform design modifications/improvements. If some significant positive features of 3D printing methodology are considered, it is correct to express that low-cost maintenance is possible, a high level of design flexibility is obtained, stable print duration is predicted, minimum waste material is formed, and sophisticated geometries are produced [1, 2]. Aside from these promising properties, the 3D printing methods can be counted as environmentally friendly due to the non-existence of any chemical reactions during production. Besides, when it is compared with the traditional production methods such as machining, casting, welding, extrusion, rolling, and powder metallurgy, AM techniques eliminate sophisticated and expensive post-processing applications and complex process planning strategies. In terms of the final products, from well-known thermoplastic polymers (ABS, PLA, and PETG) and metallic alloys (steel, aluminum, and titanium) to engineering ceramics and conventional particle reinforced composites, many different materials can be created via this useful method [3-12].

In the scientific literature, many different 3D printing techniques can be found comfortably as a consequence of rising interest in this method by researchers and engineers. Basically, AM processes are classified into two fundamental groups: fusion-based methods (fused deposition modelling, selective laser melting, electron beam melting, and laser powder bed fusion), and non-fusion-based methods (binder jet, material jet, and extrusion) [2, 13]. Considering all of these alternative methods, it can be asserted that the most widespread one is fused deposition modeling (FDM) where different thermoplastic filaments were used. In this methodology, FDM-based 3D printers work by extruding polymer filaments by means of a heated nozzle. Molten polymer flows the road controlled by the CAD program to create the end shape layer by layer. By reason of its simplicity, availability for versatile design trials, rapid fabrication time, practical maintenance, and low cost, this technique has been tried by plenty of investigators since the early appearance of additive manufacturing [14, 15]. Also, it should be emphasized that FDM provides controlling of the mechanical and physical properties by customizing the void/gap density, layer thickness, and filament building direction.

Polyethylene terephthalate glycol, which is also called as PETG, is a type of thermoplastic polymer. If the PETG is analyzed with respect to its chemical structure, it can be seen that it is a version of standard PET (polyethylene terephthalate) that has been often consumed for bottle production. With glycol addition, unique chemical features can be attained as a consequence of changed molecular pattern. This circumstance can be seen as a distinguishing property for PETG in comparison with well-known PET. Herein, it is noteworthy to express that although PET has a good potential of crystallinity resulting in poor printability, PETG minimizes this crystallinity effect altering the main body structure of the polymer chain. This situation makes it highly attractive for 3D printing applications like medical implants and tissue engineering [16].

Also, PETG exhibits some advantageous properties of cheapness, ease to finish, chemical resistance, and biocompatibility that are notably significant factors for filament selection [17]. Because of its outstanding potential for being an alternative to other widely used plastic filaments like ABS (acrylonitrile butadiene styrene) and PLA (polylactic acid), the number of scientific researches about PETG parts manufactured through FDM-based 3D printers have increased day by day. At this point, it will be true to say that the majority of the efforts aim to address surface quality, and mechanical properties (elastic modulus, tensile strength, hardness, and toughness) depending on different printing parameters.

For instance, Szykiedans et al. [18] reported that 3D printed PETG samples might exhibit mechanical anisotropy and wide range of tensile modulus. Durgashyam et al. [19] pointed out that better tensile features could be reached with minimum layer thickness and maximum infill ratio for PETG samples.

Agarwal et al. [20] produced PETG tensile samples with different orientations and indicated that layer thickness was the most decisive factor on the ultimate tensile strength.

İpekçi et al. [21] probed the effect of test vibrations on the mechanical responses of the 3D printed PETG samples and stated that lower vibration amplitudes were established at the processing speed of 3600 mm/min. Hanon et al. [22] worked on the tensile properties of additively manufactured PETG parts and the research team showed that the term mechanical anisotropy was highly important in practice. In another study,

Özen et al. [23] optimized the sample geometry so as to enhance mechanical properties of the PETG samples fabricated by FDM. Kannan et al. [24] found severe flow lines after the tensile tests in the 3D printed PETG specimens, so they recommended that samples could be improved with fiber reinforcements.

Özen et al. [25] tried to figure out the impacts of printing parameters on the mechanical properties of the PETG samples and showed that higher overlap and lower layer thickness gave rise to an increment in the elasticity modulus.

Amza et al. [26] compared 3D printed PETG and PLA samples in terms of creep behaviors and the researchers brought forward that their curves were notably similar. Bhandari et al. [27] dealt with the development of better mechanical responses of additively manufactured PETG parts and the investigation group underlined that annealing was an effective method for this purpose.

Dolyzk et al. [28] studied the fatigue behaviors of 3D printed PETG components and they put forward that longitudinal raster orientation was the best option for the highest fatigue life. In a recent effort, Eisazadeh et al. [29] reported that layer by layer fabricated PETG materials displayed a high potential in terms of elongation and toughness, which can be varied by utilizing different raster angles. When the literature studies are glanced at meticulously, it is easy to see that majority of the efforts are related to mechanical responses carried out at static or constant deformation speeds. However, it is known that mechanical properties are influenced by deformation speeds and this fact is substantially significant for real service conditions. Since PETG is utilized as orthopedic components, dental parts, antibacterial face masks, and security elements for machines, this situation is also prominent for 3D printed samples.

In this experimental effort, different from the literature efforts, the role of the test speed values on the tensile responses of PETG samples manufactured through the specific parameter adjusted FDM technique was examined depending upon different layer thicknesses. Following the manufacturing, all samples were analyzed in terms of hardness and surface roughness properties carefully. Then, uniaxial tensile tests were carried out to obtain the engineering stress-engineering strain curves. Furthermore, in order to comprehend the damage mechanism better, macroscopic and microscopic inspections were carried out on the deformed PETG samples.

2. MATERIAL AND METHOD

In this study, FDM technology which enables producing parts with complex geometry by using mostly polymer or composite filaments was used. The schematic view of the FDM technology was presented in Figure 1 below. It is known that the filament is fed into the heater and nozzle with the help of an extruder and heated up to the melting point. After that, the melted filament is deposited on the building platform according to the created g-code in FDM [30-32]. In this performance, PETG filaments procured from the Microzey Limited Company (Turkey) were used. Tensile test specimens were designed in AutoCAD 2020 program according to ASTM D638-14 Type IV standard [33], and then, all test models were saved as stl file (Figure 2a). After that, the created CAD files were transferred into the slicing program (Ultimaker Cura 4.0) to assign 3D printing parameters which were shown in Table 1 in detail (Figure 2b). Subsequently, obtained G-code information from the slicing program was sent to a 3D printer via an SD card, and lastly, PETG tensile test specimens were additively manufactured with a 3D printer (Ender Pro 3 model printer; printing size of 220x220x250 mm and printing speed of 180 mm/s) (Figure 2c). During the printing process, layer thickness values were changed although other parameters were kept constant. As layer thicknesses, 0.1, 0.2 and 0.4 mm were determined.

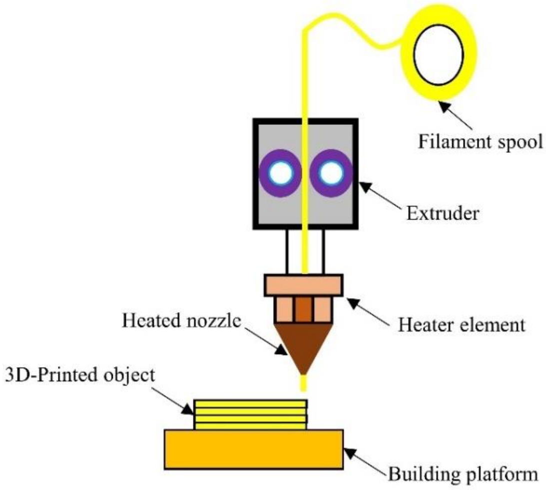

Figure 1. Schematic view of the FDM technology

In addition, no support structure was needed for manufacturing process of specimens because of having no inclined surfaces and the line pattern, which is one of the most frequently used filling patterns in the studies in the literature, was preferred. What is more, the manufacturing process was performed at the room with ambient temperature of 25 °C. Besides tensile test specimens, hardness test specimens with length of 15 mm, width of 15 mm and lastly thickness of 10 mm also were produced by using same printing parameters. The dimensions of the hardness test specimen were determined according to ASTM D2240-15 that is hardness test for polymer materials. ASTM D2240-15 standard indicates that thickness and lateral dimension of the specimens should not be lower than 6 mm and 12 mm respectively [34].

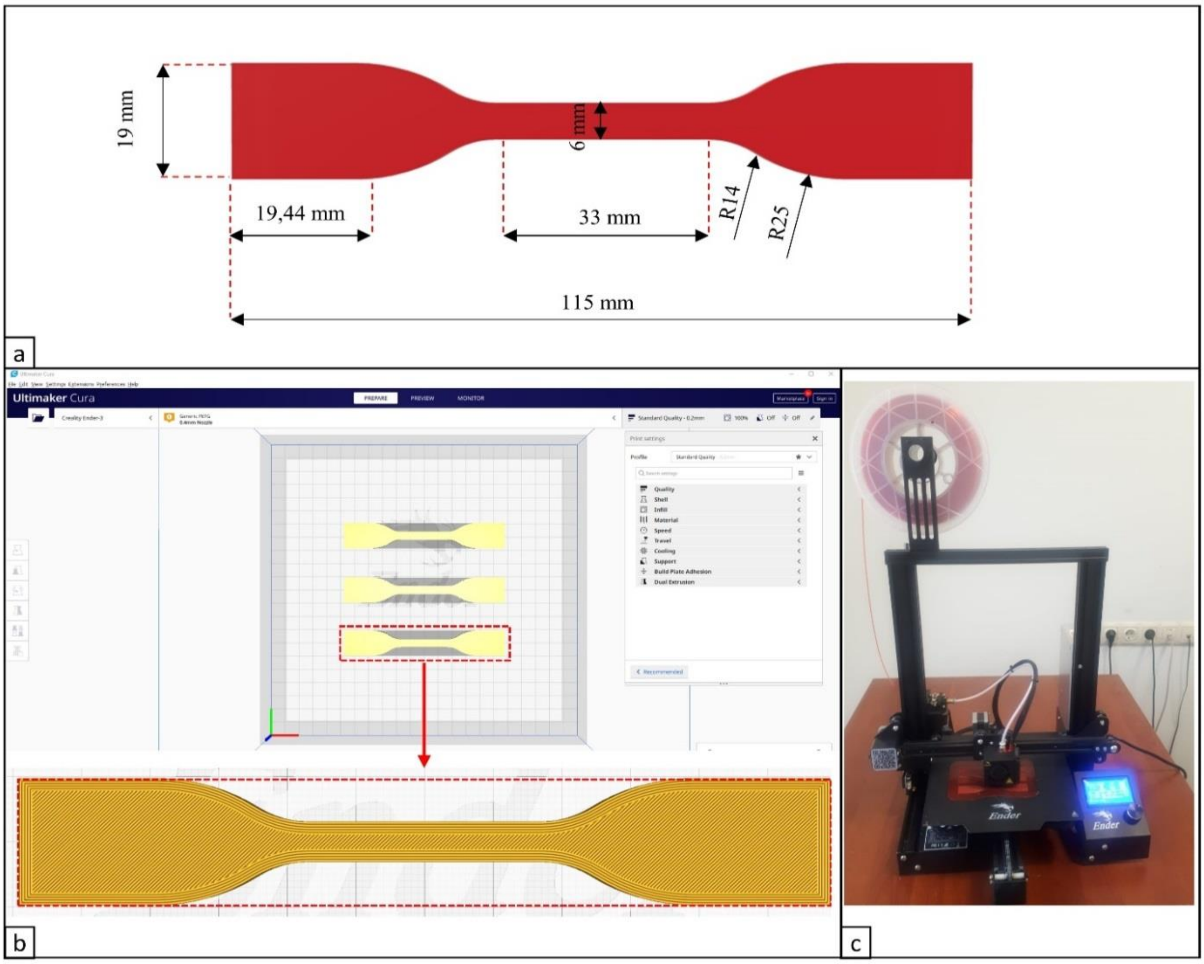

Figure 2. ASTM standard for tensile test specimens and manufacturing steps, a) Dimensions of the tensile test specimens according to ASTM D638-14 Type IV, b) View of the specimens in slicing program, c) Real view of the 3D printing process

Table 1. Printing parameters

Properties	Unit	Value
Layer thickness	*mm*	0,1; 0,2; 0,4
Infill rate	*%*	100
Infill type	-	Line
Printing speed	*mm/s*	50
Nozzle temperature	*°C*	230
Build plate temperature	*°C*	70
Raster angle	°	45/-45
Fan speed	*%*	100
Support structure	-	-

3. EXPERIMENTAL RESULTS

3.1. Hardness Measurements

Hardness measurements were carried out by means of a sensitive tester (Zwick & Co. Shore D durometer) according to ASTM D2240-15. Five different points on PETG specimens were selected and the average values were taken from these measurements. Comparative hardness results were depicted in Figure 3 below. Looking at Figure 3, it is obvious that maximum and minimum hardness values (72 Shore D and 60 Shore D) belong to the samples having the layer thickness of 0.1 mm and 0.4 mm respectively. This can be explicated by the number of stacked layers for the samples with 0.1 mm layer thickness and the good bonding capacity of the printing process.

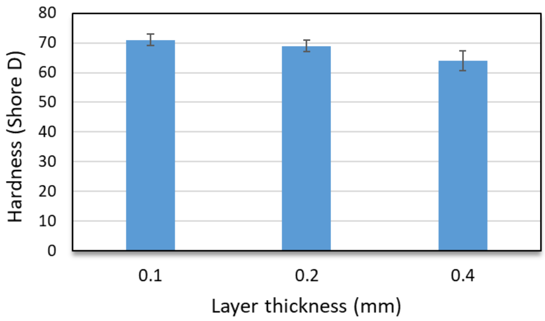

Figure 3. Hardness values of the 3D printed PETG samples

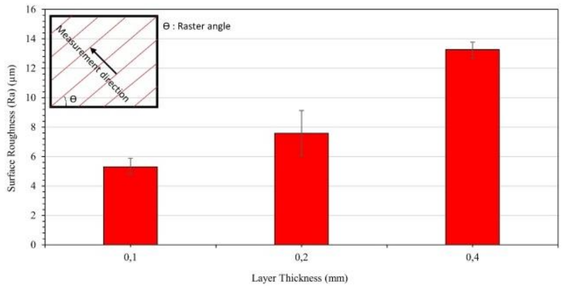

Figure 4. Measured surface roughness values depending on the layer thickness values.

3.2. Surface Roughness Analyses

The surface roughness (Ra) measurements of the top surface of the 3D printed parts were performed by using a surface roughness profilometer (Hommel Tester T500). To decide the final value of the surface roughness of the samples, five measurements were conducted perpendicular to the raster angle and obtained results were given in Figure 4.

When the Figure 4 is evaluated, it can be propounded that an increase in layer thickness values lead a rising in the surface roughness values as well. Average surface roughness values of 5.297 µm, 7.580 µm and 13.262 µm were detected for the specimens with layer thickness of 0.1 mm, 0.2 mm and 0.4 mm respectively. A similar upward trend of surface roughness values depending on increasing layer thickness values was also reported in other studies in the literature [35, 36].

In the light of measurements, it is evident that samples having 0.1 mm layer thickness exhibited better surface quality than others. This outcome is related to the number of well-packed stiff layers, and good bonding features of the manufacturing method. What's more, the highest standard deviation of 1.537 was observed during the surface roughness measurement of the specimens with 0.2 mm layer thickness. On the other hand, minimum standard deviation value of 0.515 was found for the specimens with layer thickness of 0.4 mm.

3.3. Tensile Results

Tensile tests of the 3D printed test specimens were carried out with three different test speed of 5 mm/min, 25 mm/min and 50 mm/min by using uniaxial tensile test machine (Shimadzu AG-IS; 50kN load capacity). During the mechanical tests, Trapezium 2 software was used to record the force-displacement data. Then, the collected force-displacement information was converted to engineering stress-engineering strain curves. In Figure 5, these stress-strain graphs of the tested PETG specimens can be seen in detail. Figure 5a, Figure 5b and Figure 5c exhibit the average stress-strain curves of the 3D printed PETG specimens with layer thicknesses in order of 0.1 mm, 0.2 mm and 0.4 mm. Besides, Figure 5d indicates the ultimate tensile strength with the change of layer thickness and test speed.

If the strain values were compared between all tested specimens, the highest strain of 0.1 mm/mm was observed for the specimen with a layer thickness of 0.2 mm at the test speed of 50 mm/min. On the other side, the lowest strain value of 0.06 mm/mm was detected for the specimen with 0.2 mm layer thickness at the 25 mm/min test speed. When the Figure 5d was considered, it can be pointed out that ultimate tensile strength values fluctuated by the change of test speed, and this circumstance was more apparent for increasing layer thicknesses.

Similar observations were also found by different researchers [37]. For instance, conducted tests with 25 mm/min display higher tensile strength values when compared to other test speeds if the layer thickness of 0.1 mm is evaluated. Nevertheless, the test speed of 50 mm/min and 5 mm/min leads to higher tensile strength values when the layer thickness is 0.2 mm or 0.4 mm. For 0.1 mm layer thickness, because of the fact that strong stacking effect and sufficient merging between the thin layers are present, the difference between their tensile strength values is little at different test speeds. As the layer thickness values go up to 0.4 mm, the difference can be seen easily. In addition, Figure 5d demonstrates that both the samples with 0.2 mm layer thickness and 0.4 mm layer thickness exhibit higher tensile strength levels for 50 mm/min test speed. This finding can result from the brittle deformation mechanism that was also observed in the damage analysis, and decreasing shear ability of printing layers.

If all of the data are taken into consideration, maximum average tensile strength value of 79,31 MPa was observed under 25 mm/min test speed between the specimens with layer thickness of 0.1 mm. Maximum average tensile strength value was followed by test speed of 50 mm/min with average tensile strength of 77,51 MPa and test speed of 5 mm/min with average tensile strength value of 73,70 MPa for the specimens with 0.1 mm layer thickness. For the specimens with a layer thickness of 0.2 mm, average tensile strength values of 77,58 MPa, 72,38 MPa, and 51,18 MPa were ascertained at the test speed of 50 mm/min, 5 mm/min and 25 mm/min respectively. For 0.4 mm layer thickness, the highest average tensile strength value of 69,27 MPa at 50 mm/min test speed, and the lowest average tensile strength value of 45,68 MPa at 25 mm/min test speed were determined.

Additionally, 66,89 MPa average tensile strength value was obtained for the specimen with layer thickness of 0.4 mm under 5 mm/min test speed. Another point worth mentioning is the diminishment tendency of the tensile strength values depending on increasing of the layer thickness. Especially at the test speed of 25 mm/min, the remarkable drop in tensile strength values of the specimens indicates the importance of selecting the right printing parameters for 3D printing the parts which require higher strength.

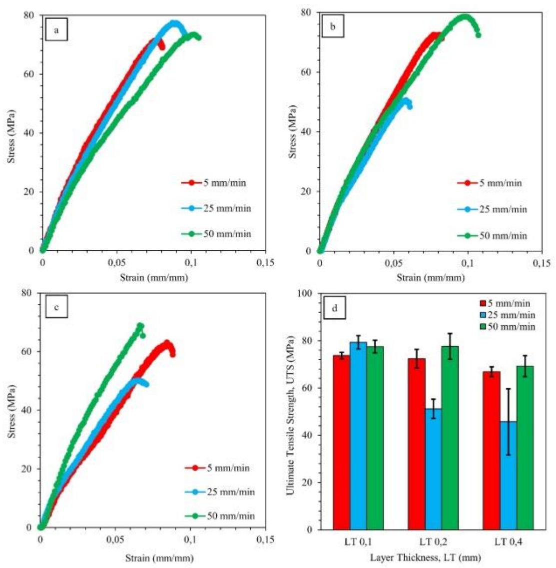

Figure 5. Stress-strain graphs depending on layer thickness and strain rate; for layer thickness: 0.1 mm(a), for layer thickness: 0.2 mm(b), for layer thickness: 0.4 mm (c), and ultimate tensile strength vs layer thickness (d)

3.4. Deformation Mechanism

After the mechanical tests, all deformed samples were analyzed in terms of their failure styles in macro and micro scales. The aim of this damage inspection is to understand the deformation better. Figure 6 and Figure 7 illustrate macro and micro (using Nikon SMZ800 stereo microscope) images of the deformed PETG samples having 0.1 mm layer thickness depending on the altering test speeds. From these images, it can be put forward that the main mechanism (extended layers along the tensile direction) is highly similar for the samples although the sample tested at 50 mm/min displays moderate brittleness (Figure 7c). That kind of damage response can be attributed to preserved elongation ability of the printing layers at lower test speeds. As the test speeds ascend to 50 mm/min level, plastic deformation and shear capability of the printing layers decline.

Figure 8 and Figure 9 show macro and micro images of the deformed PETG samples having 0.2 mm layer thickness based on the changing test speeds. From the viewpoint that emerged from these images, it can be deduced that printing layers lengthen along with the tensile direction, and deformation localized in the middle of the samples for 5 mm/min and 25 mm/min test speeds.

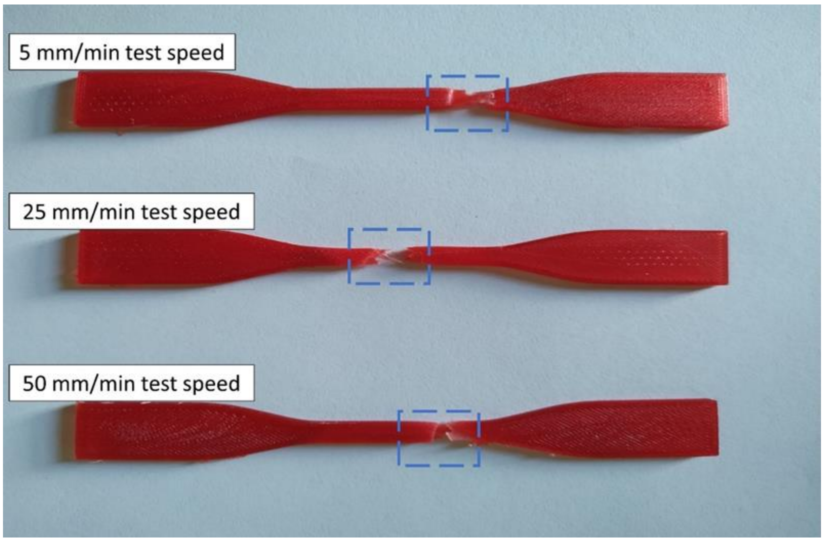

Figure 6. Macroscopic views of the deformed PETG samples having 0.1 mm layer thickness

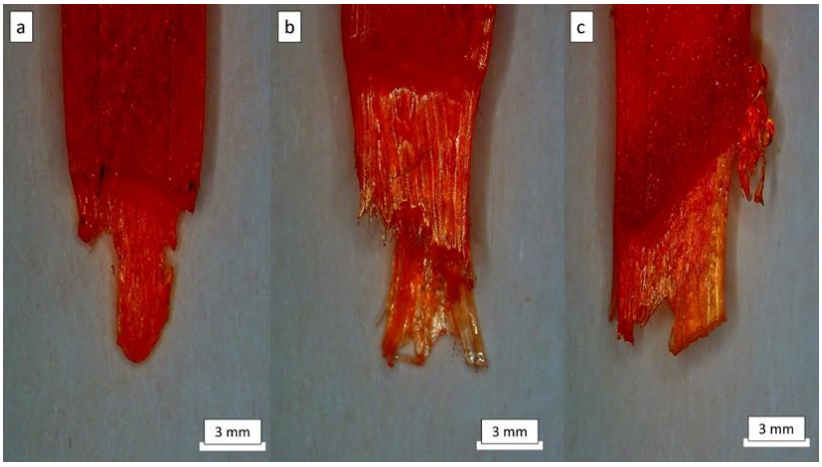

Figure 7. Optical microscope views of the deformed PETG samples having 0.1 mm layer thickness at different test speeds: 5 mm/min(a), 25 mm/min(b), and 50 mm/min(c)

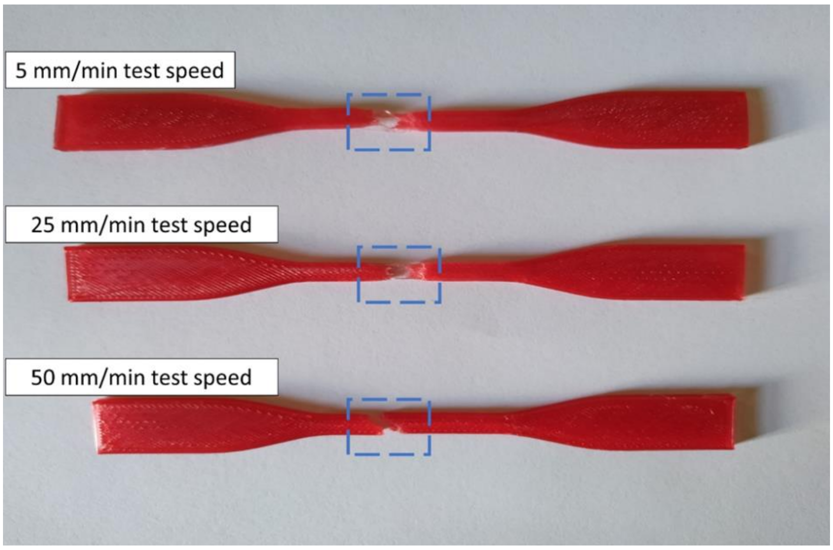

Figure 8. Macroscopic views of the deformed PETG samples having 0.2 mm layer thickness

Samples deformed at 5 mm/min behaved more ductile manner because of the fact that lower test speeds allowed easy slip of polymer chains. As the test speed reaches 50 mm/min, although the width reduction is observed on the sample, the dominant mechanism is an abrupt angular fracture (Figure 9c). Furthermore, all samples were damaged in their middle sections, and the localized deformations on the left or right sides were not established. Figure 10 and Figure 11 are macro and micro images of the deformed PETG samples having 0.2 mm layer thickness depending upon unlike test speeds. Looking at these images, it can be put forward that the main deformation emerges left and right sections of the tested specimens for 5 mm/min and 25 mm/min test speeds. Besides, for 5 mm/min and 25 mm/min test speeds, printing layers elongate vertically and break randomly, but at the test speed of 50 mm/min, slight width contraction is noticed on the sample, and the dominant mechanism, which is seen in the middle of the sample, is a brittle style angular damage.

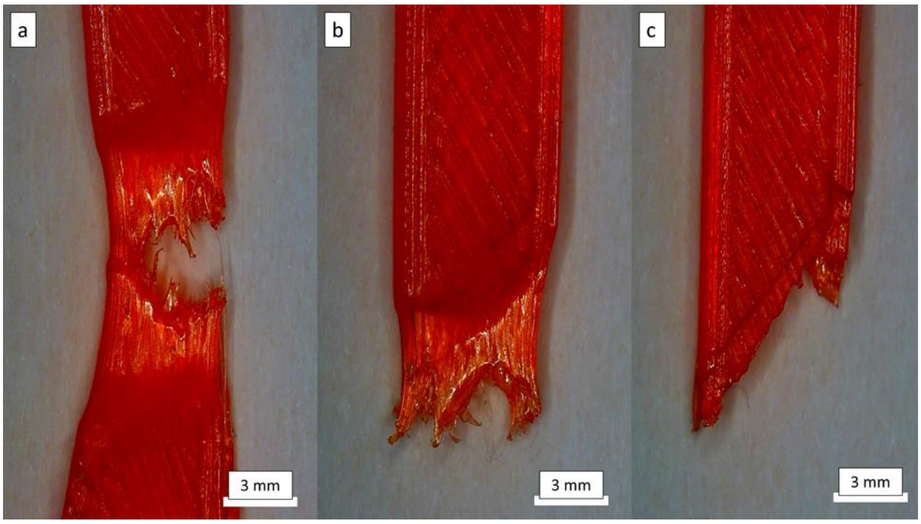

Figure 9. Optical microscope views of the deformed PETG samples having 0.2 mm layer thickness at different test speeds: 5 mm/min(a), 25 mm/min(b), and 50 mm/min(c)

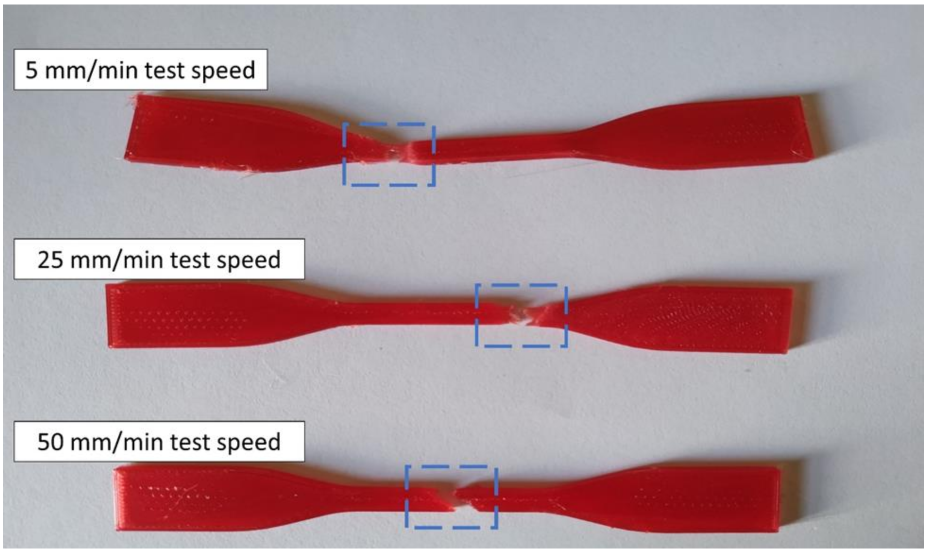

Figure 10. Macroscopic views of the deformed PETG samples having 0.4 mm layer thickness

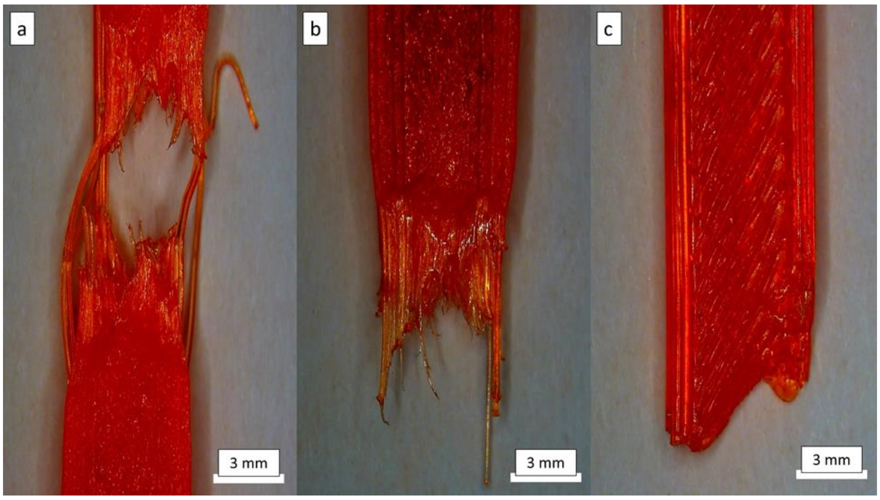

Figure 11. Optical microscope views of the deformed PETG samples having 0.4 mm layer thickness at different test speeds: 5 mm/min(a), 25 mm/min(b), and 50 mm/min(c)

4. CONCLUSIONS

As a result of this experimental study which focuses on the influence of deformation speed (5 mm/min, 25 mm/min, and 50 mm/min) on the tensile properties of the 3D printed PETG specimens with fused deposition modeling, the following outcomes can be listed;

- ✓ Using FDM printing technique proposed in this paper, flawless PETG samples satisfying the related standards with accurate dimensions could be manufactured.
- ✓ As a result of the hardness investigation, it was seen that as long as the layer thickness values of the samples decreased, measured hardness values gained a climbing tendency.
- ✓ Surface roughness measurements showed that the surface roughness values of the top surface changed with the variation of layer thickness values. The more layer thickness values were present, the poorer surface quality was obtained.
- ✓ According to tensile test results, maximum average tensile strength value of 79.31 MPa and minimum average tensile strength value of 45.68 MPa was calculated for the specimens with layer thickness of 0.1 mm and 0.4 mm respectively under the same test speed of 25 mm/min. These results showed that layer thickness affected the average tensile strength values directly due to the bonding conditions and number of stacked layers.
- ✓ From the detailed comparisons for ultimate tensile strength values depending on different test speeds, it was noticed that tensile strength values fluctuated with the change of test speed. This finding was more apparent when the layer thickness values went up.
- ✓ Regardless of their layer thickness values, all PETG samples deformed in a ductile manner at a low deformation speed of 5 mm/min. Depending on escalating test speed values, mixed-type mechanisms became significant. At the test speeds of 25 mm/min and 50 mm/min, completely brittle style damage was observed on PETG samples.

REFERENCES

1. Srinivasan, R., Nirmal Kumar, K., Jenish Ibrahim, A., Anandu, K.V., Gurudhevan R., “Impact of fused deposition process parameter (infill pattern) on the strength of PETG part”, Materials Today: Proceedings, Vol. 27, Issue 2, Pages 1801-1805, 2020.

2. Mostafaei, A., Elliott, A.M., Barnes, J.E., Li, F., Tan, W., Cramer, C.L., Nandwana, P., Chmielus, M., “Binder jet 3D printing—Process parameters, materials, properties, modeling, and challenges”, Progress in Materials Science, Vol. 119, Pages 100707, 2021.

3. Ergene, B., Şekeroğlu, İ., Bolat, Ç., Yalçın, B., “An experimental investigation on mechanical performances of 3D printed lightweight ABS pipes with different cellular wall thickness”,

Journal of Mechanical Engineering and Sciences, Vol. 15, Issue 2, Pages 8169–8177, 2021.

4. Yao, T., Deng, Z., Zhang, K., Li, S., “A method to predict the ultimate tensile strength of 3D printing polylactic acid (PLA) materials with different printing orientations”, Composites Part B: Engineering, Vol. 163, Pages 393-402, 2019.

5. Stan, F., Stanciu, N.V., Sandu, I.L., Fetecau, C., Serban, A., “Effect of low and extreme-low temperature on mechanical properties of 3D printed polyethylene terephthalate glycol copolymer”, The Romanian Journal of Technical Sciences. Applied Mechanics, Vol. 64, Issue 1, Pages 21-41, 2019.

6. Kong, D., Ni, X., Dong, C., Lei, X., Zhang, L., Man, C., Yao, J., Cheng, X., Li, X., “Bio-functional and anti-corrosive 3D printing 316L stainless steel fabricated by selective laser melting”, Materials & Design, Vol. 152, Pages 88-101, 2018.

7. Deshpande, A., Hsu, K., “Acoustoplastic metal direct-write: Towards solid aluminum 3D printing in ambient conditions”, Additive Manufacturing, Vol. 19, Pages 73-80, 2018.

8. Popov, V.V., Muller-Kamskii, G., Kovalevsky, A., Dzhenzhera, G., Strokin, E., Kolomiets, A., Ramon, J., “Design and 3D-printing of titanium bone implants: brief review of approach and clinical cases”. Biomed. Eng. Lett., Vol. 8, Pages 337–344, 2018.

9. Guo, J., Zeng, Y., Li, P., Chen, J., “Fine lattice structural titanium dioxide ceramic produced by DLP 3D printing”, Ceramics International, Vol. 45, Issue 17, Pages 23007-23012, 2019.

10. Faes, M, Valkenaers, H., Vogeler, F., Vleugels, J., Ferraris, E., “Extrusion-based 3D Printing of Ceramic Components”, Procedia CIRP, Vol. 28, Pages 76-81, 2015.

11. Zhang, X., Fan, W., Liu, T., “Fused deposition modeling 3D printing of polyamide-based composites and its applications”, Composites Communications, Vol. 21, Pages 100413, 2020.

12. Dickson, A.N., Abourayana, H.M., Dowling, D.P., “3D Printing of Fibre-Reinforced Thermoplastic Composites Using Fused Filament Fabrication—A Review”, Polymers, Vol. 12, Issue 10, Pages 2188, 2020.

13. Tuan, D. Ngo, Alireza Kashani, Gabriele Imbalzano, Kate, T.Q. Nguyen, David Hui, Additive manufacturing (3D printing): A review of materials, methods, applications and challenges, Composites Part B: Engineering, Vol. 143, Pages 172-196, 2018.

14. Popescu, D., Zapciu, A., Amza, C., Baciu, F., Marinescu, R., “FDM process parameters influence over the mechanical properties of polymer specimens: A review”, Polymer Testing, Vol. 69, Pages 157-166, 2018.

15. Garzon-Hernandez, S., Garcia-Gonzalez, D., Jérusalem, A., Arias, A., “Design of FDM 3D printed polymers: An experimental-modelling methodology for the prediction of mechanical properties”, Materials & Design, Vol. 188, Pages 108414, 2020.

16. Taniguchi, I., Yoshida, S., Hiraga, K., Miyamoto, K., Kimura, Y., Oda, K., “Biodegradation of PET: Current Status and Application Aspects”, ACS Catal., Vol. 9, Pages 4089–4105, 2019.

17. Birnfeld, H., Touguinha, G.C., Santos, R.R., Alva-Sánchez, M.S., Millão, L., “Evaluation of PETG as a material for immobilization device used in radiation therapy for head and neck”, Brazilian Journal of Radiation Sciences, Vol. 8, Issue 3, Pages 1-16, 2020.

18. Szykiedans, K., Credo, W., Osiński, D., “Selected Mechanical Properties of PETG 3-D Prints”, Procedia Engineering, Vol. 177, Pages 455-461, 2017.

19. Durgashyam, K, Reddy, M.I., Balakrishna, A., Satyanarayana, K., “Experimental investigation on mechanical properties of PETG material processed by fused deposition modeling method”, Materials Today: Proceedings, Vol. 18, Issue 6, Pages 2052-2059, 2019.

20. Agarwal, P.P., Dadmode, T.S., Kadav, M.R., Ogale, A.P., Mangave, P.P., “Experimental Analysis of Mechanical properties of PETG Material 3D Printed Material by Using Fused Deposition Modelling Technique”, Mechanical and Mechanics Engineering, Vol. 6, Issue 1, Pages 20-27, 2020.

21. Kam, M., Saruhan, H., İpekçi, A., “Investigation on the effects of 3D printer system vibrations on mechanical properties of the printed products, Sigma J Eng & Nat Sci, Vol. 36, Issue 3, Pages 655-666, 2018.

22. Hanon, M.M., Marczis, R., Zsidai, L., “Anisotropy Evaluation of Different Raster Directions, Spatial Orientations, and Fill Percentage of 3D Printed PETG Tensile Test Specimens”, KEM, Vol. 821, Pages 167–173, 2019.

23. Özen, A., Auhl, D., Völlmecke, C., Kiendl, J., Abali, B.E., “Optimization of Manufacturing Parameters and Tensile Specimen Geometry for Fused Deposition Modeling (FDM) 3D-Printed PETG”, Materials, Vol. 14, Pages 2556, 2021.

24. Kannan, S., Ramamoorthy, M., Sudhagar, E., Gunji, B., "Mechanical characterization and vibrational analysis of 3D printed PETG and PETG reinforced with short carbon fiber", AIP Conference Proceedings, Vol. 2270, Issue 1, Pages 030004, 2020.

25. Özen, A., Abali, B.E., Völlmecke, C. et al. “Exploring the Role of Manufacturing Parameters on Microstructure and Mechanical Properties in Fused Deposition Modeling (FDM) Using PETG”, Appl Compos Mater, Vol. 28, Pages 1799-1828, 2021.

26. Amza, C.G., Zapciu, A., Baciu, F., Vasile, M.I., Nicoara, A.I., “Accelerated Aging Effect on Mechanical Properties of Common 3D-Printing Polymers”, Polymers, Vol. 13, Pages 4132, 2021.

27. Bhandari, S., Lopez-Anido, R.A., Gardner, D.J., “Enhancing the interlayer tensile strength of 3D printed short carbon fiber reinforced PETG and PLA composites via annealing”, Additive Manufacturing, Vol. 30, Pages 100922, 2019.

28. Dolzyk, G., Jung, S., “Tensile and Fatigue Analysis of 3D-Printed Polyethylene Terephthalate Glycol”, J Fail. Anal. and Preven., Vol. 19, Pages 511–518, 2019.

29. Sepahi, M.T., Abusalma, H., Jovanovic, V., Eisazadeh, H., “Mechanical Properties of 3D-Printed Parts Made of Polyethylene Terephthalate Glycol”, J. of Materi Eng and Perform, Vol. 30, Pages 6851–6861, 2021.

30. Tanveer, Q., Mishra, G., Mishra, S., Sharma, R., “Effect of infill pattern and infill density on mechanical behaviour of FDM 3D printed Parts- a current review”, Materials Today: Proceedings, 2022, ISSN 2214-7853, https://doi.org/10.1016/j.matpr.2022.02.31.

31. Atakok, G., Kam, M., Koc, H.B., “Tensile, three-point bending and impact strength of 3D printed parts using PLA and recycled PLA filaments: A statistical investigation”, Journal of Materials Research and Technology, Vol. 18, Pages 1542-1554, 2022.

32. Ergene, B., Atlıhan, G., Pinar, A., “Investigation of the effect of taper angle and boundary condition on natural frequency of the 3D-Printed PET-G beams”, International Journal of 3D Printing Technologies and Digital Industry, Vol. 5, Pages 31-39, 2022.

33. ASTM D638-14. Standard test method for tensile properties of plastics. Technical Report. West Conshohocken, PA; 2014.

34. ASTM International. ASTM D2240-15e1, Standard Test Method for Rubber Property—Durometer Hardness. 2015.

35. Mat, M.A.C., Ramli, F.R., Alkahari, M.R., Sudin, M.N., Abdollah, M.F.B., Mat, S., “Influence of layer thickness and infill design on the surface roughness of PLA, PETG and metal copper materials”, Proceedings of Mechanical Engineering Research Day, Pages 64-66, 2020.

36. Ergene, B., Bolat, Ç., “An experimental study on the role of manufacturing parameters on the dry sliding wear performance of additively manufactured PETG”, International Polymer Processing, Article in Press, 2022. https://doi.org/10.1515/ipp-2022-0015.

37. Vidakis, N., Petousis, M., Velidakis, E., Liebscher, M., Mechtcherine, V., Tzounis, L., “On the Strain Rate Sensitivity of Fused Filament Fabrication (FFF) Processed PLA, ABS, PETG, PA6, and PP Thermoplastic Polymers”, Polymers, Vol. 12, Pages 2924, 2020.